Global emergent behaviors in extreme mechanics and electronics of diamond

Chang Liu,[1] Quan Li,[1,*] Yanming Ma,[1,2,†] and Changfeng Chen[3,‡]

[1]*Key Laboratory of Material Simulation Methods and Software of Ministry of Education, College of Physics, Jilin University, Changchun 130012, China*

[2]*School of Physics, Zhejiang University, Hangzhou 310027, China*

[3]*Department of Physics and Astronomy, University of Nevada, Las Vegas, Nevada 89154, USA*

(Received 26 November 2025; accepted 24 April 2026; published 7 May 2026)

Diamond is renowned for supreme hardness and supersized electronic bandgap, but knowledge is surprisingly incomplete on its prominent mechanical and electronic benchmarks under large loads. Here, using first-principles calculations, we create global mapping of extremal stress (GMES) and related strain and modulus profiles to bring out fresh perspectives on material behaviors at different scales (small versus large) and varieties (tension, compression or shear) of loads, unveiling patterns and trends of mechanical properties and record-shattering maximal stress. Moreover, we construct global mapping of electronic bandgap (GMEB) profiles to set benchmarks for rational modulation of electronic properties of diamond. This distinct protocol offers a fresh expansive view of key benchmarks beyond the prevailing paradigm, highlighting global emergent behaviors of extreme mechanics and electronics of diamond under ultimate elastic strain engineering.

DOI: 10.1103/3qhh-xcz4

I. INTRODUCTION

A central task in materials physics is to assess structural stability and its impact on broad properties. The prevailing paradigm commonly uses elastic parameters derived at small strains to set stability criteria for crystals at zero or finite hydrostatic pressure; however, stability of materials under large-strain, nonhydrostatic loads holds critical importance in dictating key mechanical benchmarks such as ultimate strength and toughness, and impacting other vital properties such as electronic bandgap. Yet, materials at large strains are much less explored. A prominent case in point is diamond, whose supreme hardness and supersized electronic bandgap are well known and widely utilized, but many of its crucial strain dependent mechanical and electronic properties are little studied and largely unknown, impeding rational pursuits of strain engineering of diamond for innovative devices.

Fundamentally, stress-strain relations connect and elucidate structural and mechanical properties [1,2]. Recent years have seen increasing interest in exploring stress responses at large strains of diverse materials and loading modes [3–23], but these studies focus on a few strain paths targeting narrowly defined problems in each case, offering little insights into broad strain dependence of material properties. Understanding such properties has become more relevant and urgent as recent advances in synthesis and characterization techniques are increasingly more capable of producing and assessing nearly defect-free specimens that exhibit structural and mechanical properties approaching the theoretical limits [24–27]. Moreover, electronic properties are sensitive to strain and undergo significant changes at large strains [28–31]. There are pressing needs to develop a robust approach to explore extreme mechanics and electronics, aiming to unveil novel phenomena and elucidate mechanisms in the emerging field of elastic strain engineering of functional materials like diamond for in-depth conceptual understanding and impactful technical applications.

In this work, we devise a protocol to better elucidate diamond under extreme strains. Using first-principles calculations, we create global mapping of extremal stress (GMES) and electronic bandgap (GMEB) profiles to unravel key mechanical and electronic benchmarks under diverse large strains up to elastic limits, offering broad and insightful perspectives on such foundational material properties. The GMES profiles reveal striking contrasts between elastic moduli derived at small strains and extremal stresses defined at large strains, and uncover steep slopes off the narrow peaks near the global maxima versus broad flat regions around the global minima of extremal stress. The results also identify a surprisingly large number of easy-slip crystal planes that are viable for formation of rich varieties of stacking faults and twin boundaries, and a record-shattering extremal stress under a previously unexplored shear deformation mode. Meanwhile, the GMEB profiles showcase load sensitive strain dependence of diamond's electronic bandgap, guiding rational design of devices with optimal strain tunability.

II. RESULTS AND DISCUSSIONS

Mapping extreme mechanical and electronic properties in broad strain space offers fresh insights into intricate trends and patterns under previously unexplored deformation modes. This work exemplifies the essence of what Philip Anderson

*Contact author: liquan777@calypso.cn
†Contact author: mym@jlu.edu.cn
‡Contact author: changfeng.chen@unlv.edu

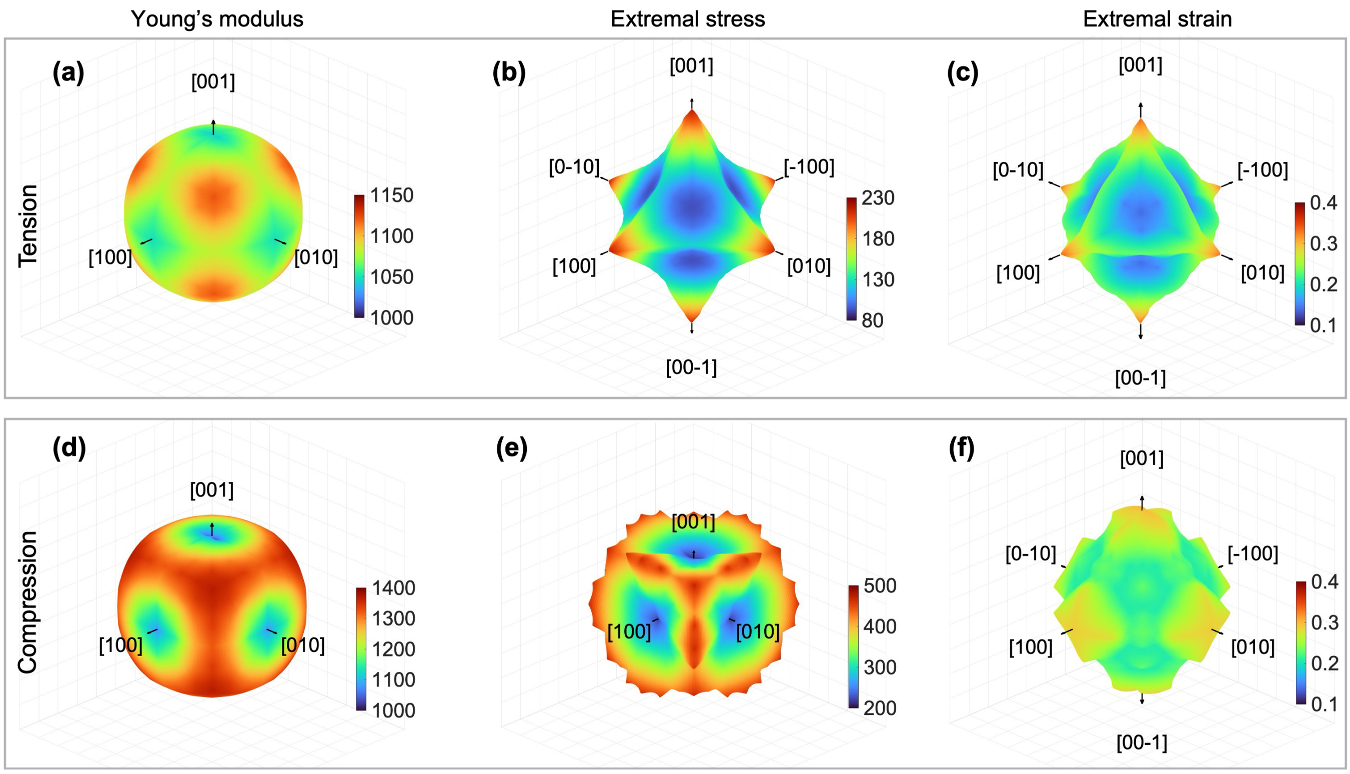

FIG. 1. The global mapping of (a) Young's modulus (scale bar in units of GPa), (b) extremal stress (scale bar in units of GPa), and (c) extremal strain of diamond under tension. The corresponding results under compression are presented in (d)–(f).

discerned in his landmark essay "More is Different" [32]: that trends and patterns arising from collection of parts can bring out a new level of emergent behaviors of the whole that cannot be seen via the limited view of individual parts. This paradigm has been widely adopted by the scientific community [33]. The present work extends this profound insight to the study of materials under extreme deformation, which is fast becoming an active research area encompassing many scientific fields. Our findings reveal global emergent behaviors in symmetries, contrasts, and extremes in strained diamond, which serves as an exemplary case of fundamental interest and aesthetic appeal with broad implications.

We compute stress-strain relations in eclectic deformation modes and verify dynamic stability of deformed diamond crystal via first-principles calculations [34], then create global mapping of elastic modulus profiles by data at small strains and extremal stress and strain profiles at large strains reaching elastic limits. The results offer fresh perspectives on global emergent behaviors of key mechanical benchmarks beyond the prevailing paradigm. In this work, we follow the established scientific practice and textbook standard to set key material benchmarks on ideal and defect-free diamond crystal, which define intrinsic material properties. Such knowledge lays the foundation for considering factors like defects and experimental constraints under diverse realistic conditions. Below we first examine the GMES profiles under tension (t-GMES) and compression (c-GMES) along with related extremal strain and Young's modulus profiles.

At small strains, stress responses to tension and compression as measured by Young's moduli show the same pattern [Figs. 1(a) and 1(d)], with global minima and maxima pointed in the ⟨001⟩ and ⟨111⟩ directions, respectively. At large strains, however, extremal stress and strain behaviors diverge under different loads. Under tension, extremal stress reaches the global maxima in the ⟨001⟩ directions [Fig. 1(b)], and declines precipitously upon directional deviations, but exhibits weak direction dependence in a large patch near the global minima in the ⟨111⟩ directions. Under compression, the extremal stress profile adopts a distinct cubical pattern [Fig. 1(e)], with the maxima occurring in the ⟨111⟩ directions at the vertices of the cubical profile, connected by high extremal stresses along the cubical edges; meanwhile, the minima occur in the ⟨001⟩ directions, each surrounded by a large flat region of low extremal stress. Interestingly, the global extremal stress and Young's modulus profiles exhibit contrasting alignments in their maxima and minima, which show opposite patterns under tension [Figs. 1(a) and 1(b)], but share the same pattern under compression [Figs. 1(d) and 1(e)], highlighting distinct stress responses at small and large strains under different loading conditions. Moreover, the extremal strain profiles show the same pattern as the extremal stress profiles under tension [Figs. 1(b) and 1(c)], but exhibit opposite patterns under compression, with the directions of the highest extremal strain aligned with those of the lowest extremal stress, and vice versa [Figs. 1(e) and 1(f)]. The largest and smallest extremal strains under tension and compression are in ⟨001⟩ and ⟨111⟩ directions [Figs. 1(c) and 1(f)], opposite to the alignments of the maximal and minimal Young's moduli [Figs. 1(a) and 1(d)].

The t-GMES, c-GMES, and related extremal strain and modulus profiles showcase complex stress-strain relations under extreme loads that are in stark contrast with and, therefore,

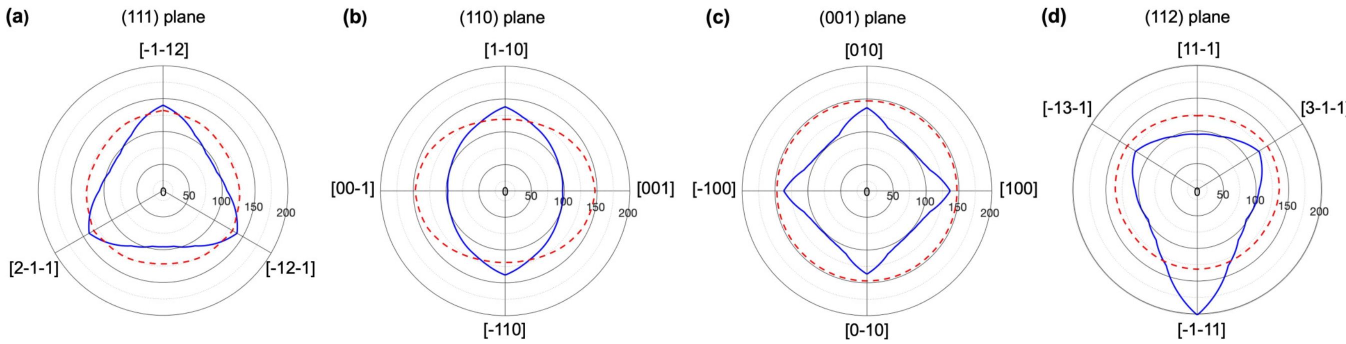

FIG. 2. The global mapping of extremal shear stress (blue solid lines) and modulus (red dashed lines, scaled by a factor 1/4) of diamond in (a) (111), (b) (110), (c) (001), and (d) (112) planes in polar coordinates. The scales up to 200 GPa (in 50 GPa intervals marked by gray circles) and the major high-symmetry crystallographic directions are indicated in each case.

cannot be derived from elastic moduli, which are obtained at small strains yet widely used in characterizing properties like hardness and toughness under extreme loads [43–55]. The present results provide a more relevant and reliable basis for predicting and analyzing physical processes and material phenomena at large strains. The emergent global behaviors of mechanical responses to large loads offer crucial insights for key property modulation via strain engineering. Our findings show that achieving maximal tensile or compressive strength in diamond requires accurate orientation control, since a slight misalignment would greatly degrade mechanical performance. Meanwhile, there exist large swaths in the crystal orientation space where extremal stresses are close to the global minimum; crystal planes normal to these directions are all likely cleavage planes [3] and are all viable for activating shear slips to promote microstructures, such as twinning, that can notably impact hardness and toughness [56]. Moreover, the knowledge of highly anisotropic extremal stress and strain offers crucial guidance for rational design and modulation of diamond structures ranging from ultrahigh-pressure anvils [57] to tunable nanoscale device components [24–27]. These insights stem from the unique global view of major benchmarks on stress-strain responses obtained via the global-mapping protocol devised in this work, which may serve as a general and robust method for unveiling material behaviors under extreme deformation. We next apply this method to study diamond under shear loads to explore behaviors in structural and mechanical properties.

Compared to tension and compression, shear produces distinct deformation modes featuring relative shifts of crystal planes. Past studies of diamond mostly focused on a few high-symmetry paths in the easy-cleavage (111) plane. Here, we construct shear GMES (s-GMES) and related modulus profiles to provide a more comprehensive view of stress responses. We first examine the shear planes normal to three principal axes. In the (111) plane, peak stresses in opposing $(111)\langle 11-2\rangle$ and $(111)\langle -1-12\rangle$ directions [Fig. 2(a)] were regarded as the high and low limits on shear stress in diamond [4,11–13]. This high anisotropy of shear stress allows microstructural engineering of mechanical properties in diamond and closely related cubic boron nitride, where densely twinned specimens exhibit greatly enhanced hardness [58,59], which was attributed to preferential bonding alignment in the stronger $(111)\langle -1-12\rangle$ direction at the twin boundaries [60,61]. Strength and toughness enhancements of similar origins also have been observed in additional covalent crystals [62–68]. Results in Fig. 2(a) reveal that deviation from the global maxima in the $(111)\langle -1-12\rangle$ direction brings about much faster stress reduction compared to the those around the global minima in the $(111)\langle 11-2\rangle$ direction, suggesting that stringent bonding alignments at twin boundaries are required to achieve optimal strength. In the meantime, in the (110) [Fig. 2(b)] and (001) [Fig. 2(c)] planes, which have been hitherto less explored, there are twofold and fourfold rotational and mirror symmetries in extremal stress distribution, compared to the threefold rotational and mirror symmetries in the (111) plane, reflecting the underlying bonding symmetries. The (110) and (001) results possess a reflection symmetry that renders the extremal stresses in every pair of opposing shear-slip directions to be identical. The highest and lowest extremal shear stresses have a ratio of 1.36 (137/101), 1.42 (138/97.4), and 1.47 (140/95.5) in the (001), (011), and (111) planes, respectively, and are aligned mutually at 45, 90, and 180 degrees, respectively, in these three planes. The highest (lowest) rate of change occurs at the stress maxima (minima), following the same pattern as seen above under tension and compression.

The t-GMES of diamond [Fig. 1(c)] shows that its extremal tensile stress stays close to global minima in large swaths of orientation space near $\langle 111\rangle$ directions, suggesting that ample (lmn) planes with $l \approx m \approx n$, close to (111), are viable cleavage planes [3] and, more importantly, prime slip planes to form stacking faults or twin boundaries. We examined many such shear planes and found similar extremal stresses as in the (111) plane. A conspicuous case, however, is the (112) plane [Fig. 2(d)], which hosts extremal stresses with stark disparity, with a lower minimal peak yet remarkably higher maximal peak shear stress reaching 202 GPa in the $(112)\langle -1-11\rangle$ direction. This is one of the largest known shear stresses in any material, well surpassing the prior record of 140 GPa in diamond under the $(111)\langle -1-12\rangle$ shear [4]. The stress anisotropy in the (112) plane, as measured by the ratio of the highest to lowest extremal stresses, 2.14 (202/94.5), is much larger than those in the low-index planes, greatly expanding the range of extremal shear stress in diamond.

The findings from the s-GMES profiles hold major significance for microstructural tuning of strength and hardness of diamond. A recent study reported [67] unprecedented

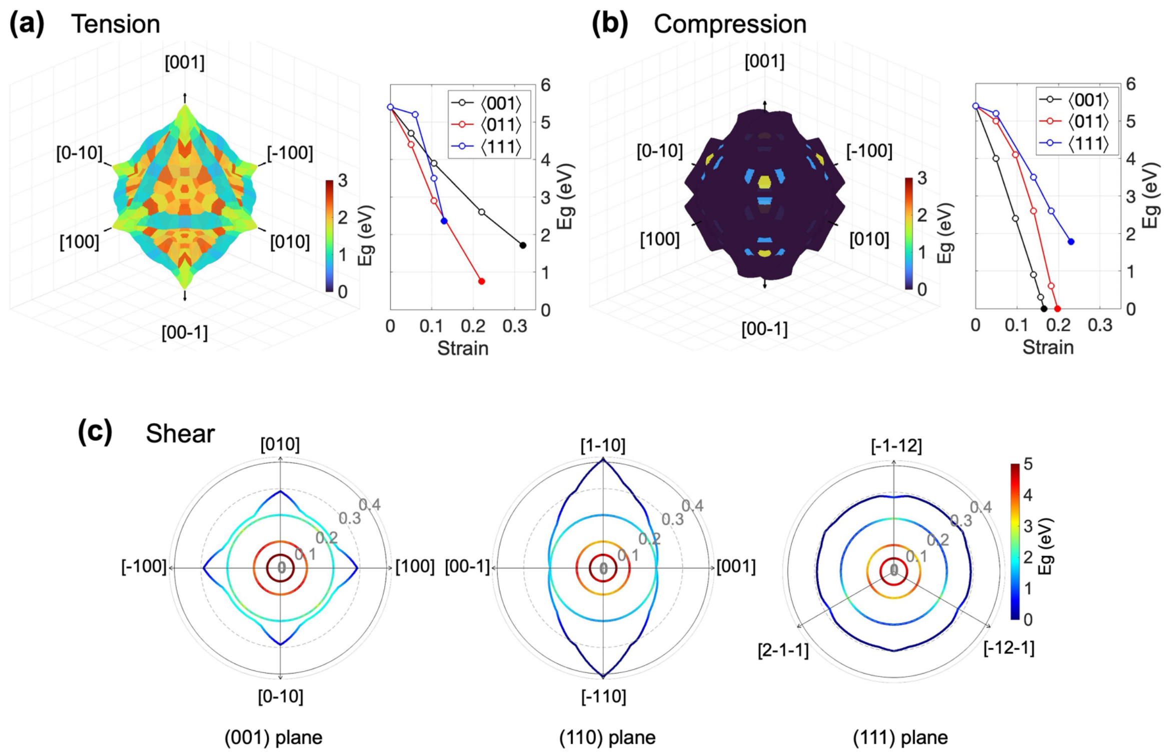

FIG. 3. The GMEB profiles under (a) tension and (b) compression, mapped onto the extremal strain profiles [Figs. 1(c) and 1(f)], and (c) shear, at 0.05, 0.1, 0.2 strains (three inner colored contours) and at the elastic limit (outermost colored contour). Bandgap (E_g) data up to maximal strains (solid symbols) on three low-index paths are shown in right panels in (a) and (b).

hardness in diamond composites with refined nanotwins. Our results provide insights into the underlying atomistic mechanism by unveiling the directional deformation mode, which is capable of generating significantly increased stress response [4], to sustain much enhanced hardness via favorable twinning structures [60,61]. It establishes a microscopic origin for the extraordinary mechanical performance of the diamond composites in which twin boundaries help generate superior strength and hardness. Moreover, all the s-GMES profiles exhibit extremal stress distributions at large strains in sharp contrast with the shear moduli derived at small strains. Shear moduli are among the primary parameters widely used as input in empirical formulas to estimate hardness and toughness [43–55], but these prominent mechanical benchmarks are determined at large strains and thus better described by extremal stresses [3–23]. The s-GMES profiles are therefore expected to offer a more comprehensive and accurate description of these key benchmarks.

Understanding mechanical properties at large strains requires knowledge of stress-strain relations approaching eclectic elastic limits. This work aims to construct extremal profiles that set intrinsic benchmarks and constrain measured values on high-quality samples [24–27]. More broadly, such extreme mechanics establish a foundation for probing global emergent behaviors in the full strain space, which has hitherto been much less explored compared to material behaviors near strain-free equilibrium conditions. In particular, stress responses at large strains provide a sound basis to extend and possibly improve previously developed and widely applied formulas and analysis largely derived from elastic moduli determined at small strains near equilibrium conditions.

We now create GMEB profiles of diamond. Past studies examined bandgaps in silicon and diamond at empirically chosen strains [69,70], but it remains an outstanding task to determine the bandgap tunability in ultimate elastically tuned diamond. Here we assess bandgap of diamond on broad GMEB profiles and also along selected key strain paths [34]. Under tension [Fig. 3(a)], bandgap remains finite on the GMEB profile, undergoing sharp decline and reaching the lowest value (<1.0 eV) in the vicinity of the ⟨011⟩ direction. Meanwhile, in large swaths around the ⟨111⟩ directions, bandgaps retain the highest values above 2.5 eV on the GMEB profile, limited by the smallest maximal strains [Fig. 1(d)]. Surprisingly, in the ⟨001⟩ directions, the bandgap stays high (above 1.5 eV), despite the largest maximal strain [Fig. 1(d)]. These findings reveal sensitive and intriguing direction dependence of bandgap in ultimate elastically strained diamond and provide guidance for rational device design and load management for functional optimization. In contrast, under compression, bandgap responses to strains exhibit different behaviors both in variation rates and in relative directional dependence. Especially noteworthy is that the GMEB profile [Fig. 3(b)] goes almost completely dark, indicating full bandgap closure in nearly all parts of orientation space. The ⟨001⟩ compression, with the lowest maximal stress [Fig. 1(g)], produces the fastest bandgap reduction. This global view of bandgap variation is indispensable to optimal strain tuning of bandgap in diamond. Finally, under shear, bandgap exhibits high direction sensitivity and closes within the elastic limits under favorable shear deformation modes [Fig. 3(c)].

The principles of stress induced bandgap changes have been long established; for example, early studies elucidated symmetry breaking induced bandgap reduction in diamond under anisotropic stress [71]. What has been missing, however, is bandgap evolution behaviors under diverse deformation modes, which have been hitherto little explored. In this work we probe bandgap profiles in deformed diamond under diverse large strains approaching distinct elastic limits. The results offer fresh insights into the intriguing trends and patterns of bandgap variations in broad strain space. Such results may guide effective elastic strain engineering and optimize functional tuning strategies. While detailed material and load dependent behaviors still need to be worked out for specific cases, the present results unveil both qualitative (trends, patterns, symmetries) and quantitative (magnitudes, limits) attributes that set the foundation for device design and performance optimization.

III. SUMMARY

In summary, we have devised a GMES-GMEB protocol to probe structural, mechanical, and electronic properties of ultimate elastically strained diamond. The results bring out fresh perspectives of fundamental interest and aesthetic appeal, showcasing, on distinct and broad scale, congruent versus contrasting symmetries in key benchmarks, consistency versus disparity in directional alignments of extremal quantities, and steep versus flat rates of changing properties. Notable findings include (i) stark differences in orientation dependence of elastic moduli and extremal stresses, highlighting distinct stress responses at small, and large strains; (ii) sharp contrasts in stress variation rates near global maxima and minima, offering insights for optimal stress modulation; (iii) surprisingly close extremal stresses in wide swaths of the t-GMES profile, revealing ample easy-slip shear planes for effective microstructural engineering; (iv) unexpectedly high anisotropy in select s-GMES profiles with the record-shattering maximal shear stress, elucidating superior strength and hardness in diamond nanocomposites; and (v) diverse paths and wide ranges of tuning electronic bandgap under eclectic deformation modes, guiding rational device design. This paradigm appraises structure-property relations via an expansive global view beyond the prevailing knowledge stemming from individual strain paths. Our findings exemplify the profound perspective of "More is Different" [32,33] in the fresh context of extreme mechanics and electronics of diamond, which is an exceptional material that has long drawn enormous interest from fundamental research and practical application, and has served as an exemplary case to provide broad insights for elucidating many materials adopting the same crystal structure and bonding type.

ACKNOWLEDGMENTS

This work was supported by the National Natural Science Foundation of China (Grants No. 12202158, No. 12574016, No. T2325013, No. 52288102, and No. 52090024) and the Science and Technology Development Program of Jilin province (Grant No. 20250101039JJ).

DATA AVAILABILITY

The data that support the findings of this article are not publicly available upon publication because it is not technically feasible and/or the cost of preparing, depositing, and hosting the data would be prohibitive within the terms of this research project. The data are available from the authors upon reasonable request.

[1] D. Roundy, C. R. Krenn, M. L. Cohen, and J. W. Morris Jr., Ideal shear strengths of fcc aluminum and copper, Phys. Rev. Lett. **82**, 2713 (1999).
[2] J. W. Morris Jr. and C. R. Krenn, The internal stability of an elastic solid, Philos. Mag. A **80**, 2827 (2000).
[3] R. H. Telling, C. J. Pickard, M. C. Payne, and J. E. Field, Theoretical strength and cleavage of diamond, Phys. Rev. Lett. **84**, 5160 (2000).
[4] H. Chacham and L. Kleinman, Instabilities in diamond under high shear stress, Phys. Rev. Lett. **85**, 4904 (2000).
[5] S. H. Jhi, S. G. Louie, M. L. Cohen, and J. W. Morris Jr., Mechanical instability and ideal shear strength of transition metal carbides and nitrides, Phys. Rev. Lett. **87**, 075503 (2001).
[6] S. Ogata, J. Li, and S. Yip, Ideal pure shear strength of aluminum and copper, Science **298**, 807 (2002).
[7] D. M. Clatterbuck, C. R. Krenn, M. L. Cohen, and J. W. Morris Jr., Phonon instabilities and the ideal strength of aluminum, Phys. Rev. Lett. **91**, 135501 (2003).
[8] D. M. Clatterbuck, D. C. Chrzan, and J. W. Morris Jr., The influence of triaxial stress on the ideal tensile strength of iron, Scr. Mater. **49**, 1007 (2003).
[9] S. Ogata, J. Li, N. Hirosaki, Y. Shibutani, and S. Yip, Ideal shear strain of metals and ceramics, Phys. Rev. B **70**, 104104 (2004).
[10] X. Blase, P. Gillet, A. San Miguel, P. Melinon, Exceptional ideal strength of carbon clathrates, Phys. Rev. Lett. **92**, 215505 (2004).
[11] Y. Zhang, H. Sun, and C. F. Chen, Superhard cubic BC_2N compared to diamond, Phys. Rev. Lett. **93**, 195504 (2004).
[12] Y. Zhang, H. Sun, and C. F. Chen, Atomistic deformation modes in strong covalent solids, Phys. Rev. Lett. **94**, 145505 (2005).
[13] Y. Zhang, H. Sun, and C. F. Chen, Structural deformation, strength, and instability of cubic BN compared to diamond: A first-principles study, Phys. Rev. B **73**, 144115 (2006).
[14] M. G. Fyta, I. N. Remediakis, P. C. Kelires, and D. A. Papaconstantopoulos, Insights into the fracture mechanisms and strength of amorphous and nanocomposite carbon, Phys. Rev. Lett. **96**, 185503 (2006).
[15] R. F. Zhang, S. Veprek, and A. S. Argon, Anisotropic ideal strengths and chemical bonding of wurtzite BN in comparison to zincblende BN, Phys. Rev. B **77**, 172103 (2008).
[16] Q. Li, D. Zhou, W. Zheng, Y. Ma, and C. Chen, Anomalous stress response of ultrahard WB_n compounds, Phys. Rev. Lett. **115**, 185502 (2015).

[17] C. Lu, Q. Li, Y. Ma, and C. Chen, Extraordinary indentation strain stiffening produces superhard tungsten nitrides, Phys. Rev. Lett. **119**, 115503 (2017).

[18] S. Guo and H. Sun, Superhardness induced by grain boundary vertical sliding in (001)-textured ZrB_2 and TiB_2 nano films, Acta Mater. **218**, 117212 (2021).

[19] C. Liu, X. Gao, K. Zhang, W. Zheng, and C. Chen, Exceptional strain strengthening and tuning of mechanical properties of TiN, Phys. Rev. B **106**, 054112 (2022).

[20] C. Liu, X. Gu, K. Zhang, W. Zheng, Y. Ma, and C. Chen, Superhard metallic compound TaB_2 via crystal orientation resolved strain stiffening, Phys. Rev. B **105**, 024105 (2022).

[21] H. Lv, X. Gao, K. Zhang, M. Wen, X. He, Z. Wu, C. Liu, C. Chen, and W. Zheng, Bamboo-like dual-phase nanostructured copper composite strengthened by amorphous boron framework, Nat. Commun. **14**, 4836 (2023).

[22] J. Pan, K. Zhang, J. Wang, X. Gu, Q. Zhao, Y. Shan, M. Wen, C. Liu, W. Zheng, and C. Chen, Macroscale ultradurable superlubricity on passivated transition-metal diborides, Acta Mater. **262**, 119439 (2024).

[23] X. Gao, K. Zhang, Q. Zhu, C. Chen, and C. Liu, Setting material benchmarks at large-strain limits via ultimate strengths, Acta Mater. **286**, 120724 (2025).

[24] H. Zhang, J. Tersoff, S. Xu, H. Chen, Q. Zhang, K. Zhang, Y. Yang, C. Lee, K. Tu, J. Li, and Y. Lu, Approaching the ideal elastic strain limit in silicon nanowires, Sci. Adv. **2**, e1501382 (2016).

[25] A. Banerjee, D. Bernoulli, H. Zhang, M. F. Yuen, J. Liu, J. Dong, F. Ding, J. Lu, M. Dao, W. Zhang, Y. Lu, and S. Suresh, Ultralarge Elastic Deformation of Nanoscale Diamond, Ultralarge elastic deformation of nanoscale diamond, Science **360**, 300 (2018).

[26] A. Nie, Y. Bu, P. Li, Y. Zhang, T. Jin, J. Liu, Z. Su, Y. Wang, J. He, Z. Liu, H. Wang, Y. Tian, and W. Yang, Approaching diamond's theoretical elasticity and strength limits, Nat. Commun. **10**, 5533 (2019).

[27] C. Dang, J. Chou, B. Dai, C. Chou, Y. Yang, R. Fan, W. Lin, F. Meng, A. Hu, J. Zhu, J. Han, A. M. Minor, J. Li, and Y. Lu, Achieving large uniform tensile elasticity in microfabricated diamond, Science **371**, 76 (2021).

[28] C. Liu, X. Song, Q. Li, Y. Ma, and C. Chen, Smooth flow in diamond: Atomistic ductility and electronic conductivity, Phys. Rev. Lett. **123**, 195504 (2019).

[29] C. Liu, X. Song, Q. Li, Y. Ma, and C. Chen, Superconductivity in compression-shear deformed diamond, Phys. Rev. Lett. **124**, 147001 (2020).

[30] C. Liu, X. Song, Q. Li, Y. Ma, and C. Chen, Superconductivity in Shear Strained Semiconductors, Superconductivity in Shear Strained Semiconductors, Chin. Phys. Lett. **38**, 086301 (2021).

[31] X. Song, C. Liu, Q. Li, R. J. Hemley, Y. Ma, and C. Chen, Stress-induced high-T_c superconductivity in solid molecular hydrogen, Proc. Natl. Acad. Sci. USA **119**, e2122691119 (2022).

[32] P. W. Anderson, More is different, Science **177**, 393 (1972).

[33] S. Strogatz, S. Walker, J. M. Yeomans, C. Tarnita, E. Arcaute, M. De Domenico, O. Artime, and K. Goh, Fifty years of 'more is different,' Nat. Rev. Phys. **4**, 508 (2022).

[34] We used the VASP code [35], adopting the PAW potentials [36], LDA functional by Ceperley and Alder (LDA-CA) [37] and a plane-wave basis set. An energy cutoff of 800 eV and a Monkhorst-Pack grid [38] with a maximum spacing of $2\pi \times 0.02$ Å^{-1} achieved energy, stress, and force convergence of 1 meV/atom, 0.1 GPa and 0.005 eV/Å, respectively. A quasistatic stress relaxation procedure was used to generate peak stress and strain [11–13]. Dynamic stability of the deformed crystal was evaluated by calculating phonon dispersion via the finite displacements in supercell method using the Phonopy package [39,40]. Electronic bandgaps were calculated using the Heyd-Scuseria-Ernzerhof (HSE) hybrid functional [41,42].

[35] G. Kresse and L. Furthmüller, Efficient iterative schemes for ab initio total-energy calculations using a plane-wave basis set, Phys. Rev. B **54**, 11169 (1996).

[36] G. Kresse and D. Joubert, From ultrasoft pseudopotentials to the projector augmented-wave method, Phys. Rev. B **59**, 1758 (1999).

[37] D. M. Ceperley and B. J. Alder, Ground state of the electron gas by a stochastic method, Phys. Rev. Lett. **45**, 566 (1980).

[38] H. J. Monkhorst and J. D. Pack, Special points for brillouin-zone integrations, Phys. Rev. B **13**, 5188 (1976).

[39] A. Togo, First-principles phonon calculations with Phonopy and Phono3py, J. Phys. Soc. Jpn. **92**, 012001 (2023).

[40] A. Togo, L. Chaput, T. Tadano, and I. Tanaka, Implementation strategies in phonopy and phono3py, J. Phys.: Condens. Matter **35**, 353001 (2023).

[41] J. Heyd, G. E. Scuseria, and M. Ernzerhof, Hybrid functionals based on a screened Coulomb potential, J. Chem. Phys. **118**, 8207 (2003).

[42] J. Heyd, G. E. Scuseria, and M. Ernzerhof, Erratum: Hybrid functionals based on a screened Coulomb potential, J. Chem. Phys. **124**, 219906 (2006).

[43] S. F. Pugh, Relations between the elastic moduli and the plastic properties of polycrystalline pure metals, London, Edinburgh, Dublin Philos. Mag. J. Sci. **45**, 823 (1954).

[44] A. Y. Liu and M. L. Cohen, Prediction of new low compressibility solids, Science **245**, 841 (1989).

[45] D. G. Pettifor and M. Aoki, Bonding and structure of intermetallics: A new bond order potential, Philos. Trans. R. Soc., A **334**, 439 (1991).

[46] D. G. Pettifor, Theoretical predictions of structure and related properties of intermetallics, Mater. Sci. Technol. **8**, 345 (1992).

[47] F. Gao, J. He, E. Wu, S. Liu, D. Yu, D. Li, S. Zhang, and Y. Tian, Hardness of covalent crystals, Phys. Rev. Lett. **91**, 015502 (2003).

[48] A. Šimůnek and J. Vackář, Hardness of covalent and ionic crystals: First-principle calculations, Phys. Rev. Lett. **96**, 085501 (2006).

[49] K. Balasubramanian, S. V. Khare, and D. Gall, Valence electron concentration as an indicator for mechanical properties in rocksalt structure nitrides, carbides and carbonitrides, Acta Mater. **152**, 175 (2018).

[50] X. L. Gu, C. Liu, H. Guo, K. Zhang, and C. F. Chen, Sorting transition-metal diborides: New descriptor for mechanical properties, Acta Mater. **207**, 116685 (2021).

[51] D. M. Teter and R. J. Hemley, Low-compressibility carbon nitride, Science **271**, 53 (1996).

[52] D. M. Teter, Computational alchemy: The search for new superhard materials, MRS Bull. **23**, 22 (1998).

[53] K. Li, X. Wang, F. Zhang, and D. Xue, Electronegativity identification of novel superhard materials, Phys. Rev. Lett. **100**, 235504 (2008).

[54] X. Chen, H. Niu, D. Li, and Y. Li, Modeling hardness of polycrystalline materials and bulk metallic glasses, Intermetallics **19**, 1275 (2011).
[55] Y. Tian, B. Xu, and Z. Zhao, Microscopic theory of hardness and design of novel superhard crystals, Int. J. Refract. Met. Hard Mater. **33**, 93 (2012).
[56] A. M. Nie, Z. S. Zhao, B. Xu, and Y. J. Tian, Microstructure engineering in diamond-based materials, Nat. Mater. **24**, 1172 (2025).
[57] B. Li, C. Ji, W. Yanga, J. Wang, K. Yang, R. Xu, W. Liu, Z. Cai, J. Chen, and H. K. Mao, Diamond anvil cell behavior up to 4 Mbar, Proc. Natl. Acad. Sci. USA **115**, 1713 (2018).
[58] Y. Tian, B. Xu, D. Yu, Y. Ma, Y. Wang, Y. Jiang, W. Hu, C. Tang, Y. Gao, K. Luo, Z. Zhao, L. M. Wang, B. Wen, J. He, and Z. Liu, Ultrahard nanotwinned cubic boron nitride, Ultrahard nanotwinned cubic boron nitride, Nature (London) **493**, 385 (2013).
[59] Q. Huang, D. Yu, B. Xu, W. Hu, Y. Ma, Y. Wang, Z. Zhao, B. Wen, J. He, Z. Liu, and Y. Tian, Nanotwinned diamond with unprecedented hardness and stability, nanotwinned diamond with unprecedented hardness and stability, Nature (London) **510**, 250 (2014).
[60] B. Li, H. Sun, and C. F. Chen, Large indentation strain-stiffening in nanotwinned cubic boron nitride, Nat. Commun. **5**, 4965 (2014).
[61] B. Li, H. Sun, and C. F. Chen, Extreme mechanics of probing the ultimate strength of nanotwinned diamond, Phys. Rev. Lett. **117**, 116103 (2016).
[62] Z. C. Pan, H. Sun, and C. F. Chen, Colossal shear-strength enhancement of low-density cubic BC_2N by nanoindentation, Phys. Rev. Lett. **98**, 135505 (2007).
[63] Z. C. Pan, H. Sun, and C. F. Chen, Harder than diamond: Superior indentation strength of wurtzite BN and lonsdaleite, Phys. Rev. Lett. **102**, 055503 (2009).
[64] Y. Yue, Y. Gao, W. Hu, B. Xu, J. Wang, X. Zhang, Q. Zhang, Y. Wang, B. Ge, Z. Yang, Z. Li, P. Ying, X. Liu, D. Yu, B. Wei, Z. Wang, X. Zhou, L. Guo, and Y. Tian, Hierarchically structured diamond composite with exceptional toughness, Nature (London) **582**, 370 (2020).
[65] K. Luo, B. Liu, W. Hu, X. Dong, Y. Wang, Q. Huang, Y. Gao, L. Sun, Z. Zhao, Y. Wu, Y. Zhang, M. Ma, X. Zhou, J. He, D. Yu, Z. Liu, B. Xu, and Y. Tian, Coherent interfaces govern direct transformation from graphite to diamond, Nature (London) **607**, 486 (2022).
[66] Y. Wu, Y. Zhang, X. Wang, W. Hu, S. Zhao, T. Officer, K. Luo, K. Tong, C. Du, L. Zhang, B. Li, Z. Zhuge, Z. Liang, M. Ma, A. Nie, D. Yu, J. He, Z. Liu, B. Xu, Y. Wang, *et al.*, Twisted-layer boron nitride ceramic with high deformability and strength, Nature (London), **626**, 779 (2024).
[67] P. Ying, B. Li, M. Ma, Y. Gao, R. Sun, Z. Li, S. Chen, B. Zhang, H. Li, B. Liu, L. Sun, S. Zhao, K. Tong, W. Hu, Y. Pan, G. Tang, D. Yu, Z. Zhao, B. Xu, and Y. Tian, Enhancing the hardness of diamond through twin refinement and interlocked twins, Nat. Synth. **4**, 391 (2025).
[68] C. Wang, Z. Li, Y. Cheng, X. Weng, Y. Bu, K. Zhai, T. Xue, H. Yuan, A. Nie, X. Zhou, H. Wang, Y. Tian, and Z. Liu, Reversible shuffle twinning yields anisotropic tensile superelasticity in ceramic GeSe, Nat. Nanotechnol. **20**, 732 (2025).
[69] Z. Shi, E. Tsymbalov, M. Dao, S. Suresh, A. Shapeev, and J. Li, Deep elastic strain engineering of bandgap through machine learning, Proc. Natl. Acad. Sci. USA **116**, 4117 (2019).
[70] Z. Shi, M. Dao, E. Tsymbalov, A. Shapeev, J. Li, and S. Suresh, Metallization of diamond, Proc. Natl. Acad. Sci. USA **117**, 24634 (2020).
[71] M. P. Surh, S. G. Louie, and M. L. Cohen, Band gaps of diamond under anisotropic stress, Phys. Rev. B **45**, 8239 (1992).